Viscoelastic Modeling and Inversion of a Marine Data Set

Susan E. Minkoff* **William W. Symes***

June 23, 1994

Summary

Deterministic waveform inversion in the $p - \tau$ domain permits estimation of the long-wavelength p-wave background velocity, the short-wavelength elastic parameter fluctuations, and the energy source for a marine data set from the Gulf of Mexico. The forward map is a convolutional model for p-wave primaries-only seismograms of viscoelastic, layered media. Two types of inversion (output least squares and differential semblance optimization) allow efficient estimation of various parameter combinations. Background velocities computed by differential semblance optimization were as consistent kinematically as those produced by interactive migration velocity analysis and gave somewhat more accurate depths. Source parameters obtained by output least squares inversion permitted considerably better fit to data than did those produced by an air gun modeling package. Output least squares inversion gave very short-scale detail of major reflectors closely resembling the detail derived from well logs. Despite evidence of considerable lateral heterogeneity in the shallow subsurface, estimates of deeper reflectors were remarkably consistent from midpoint to midpoint.

Introduction

Seismic inversion of real data has become increasingly successful as more sophisticated forward modeling techniques are used. Recent references which describe some of these models include [IGEL, 1993] (and references therein) and [MARTINEZ and MCMECHAN, 1991]. In his thesis, Igel discusses numerical experiments performed on the same marine data set used in this paper. Igel

*The Rice Inversion Project, Department of Computational and Applied Mathematics, Rice University, Houston TX 77251-1892

inverts for the p-wave impedance and Poisson's ratio using a two-dimensional elastic finite difference simulator. Martinez and McMechan use plane-wave, layered-medium viscoelastic modeling to estimate quality factors, shear and compressional wave velocities and the density. In neither case is the energy source estimated *via inversion*, and in Igel's work the long-wavelength background velocity is assumed known as well. Other recent inversion references which use an elastic model for wave propagation through the earth include [PAN et al., 1993] and [WOOD, 1993]. Again, the energy source is determined via statistical means and assumed known throughout the inversion. Classic techniques for estimating the energy source include predictive deconvolution (see [ROBINSON, 1967]) and homomorphic deconvolution (for an example see [ULRYCH, 1971]). The use of inversion to estimate the energy source and elastic parameters is described in [MINKOFF and SYMES, 1993], and references cited there.

Using a viscoelastic model for primary plane-wave reflections in a layered earth, we inverted a real $p - \tau$ marine data set from the Gulf of Mexico. Our work is different from all previous work described in the references above in that we used waveform inversion to estimate velocities, modeled attenuation and three dimensional amplitudes, and estimated the energy source via inversion. The numerical experiments detailed in this paper suggest that our inversion technique and viscoelastic modeler produced kinematically accurate background velocities. The estimates of the energy source and elastic parameter reflectivities appear to be improvements over initial estimates of these parameters from migration velocity analysis and an air gun modeling package.

In order to present the numerical experiments discussed in the last half of the paper, we start by describing the viscoelastic convolutional p-wave seismogram model. The next section details the inversion algorithms used to estimate the parameters in our model, and finally we present the geometry and preprocessing of the marine data set.

The Viscoelastic Convolutional Model

We model the earth as a viscoelastic medium. The mechanical parameters in the model include the density, ρ, the shear and compressional wave velocities, v_S and v_P, and the shear and compressional quality factors, q_S and q_P. The time-dependent, anisotropic source is assumed to have, approximately, point support.

Assume that the earth is a layered medium. Thus the parameters in our model vary only with depth, $z \equiv x_3$. By applying the Radon integral transform (or plane-wave decomposition) to the solution of the viscoelastic wave equation (and to common midpoint gathers of the data) we reduce the three-dimensional model to a family of one-dimensional models (see [TREITEL et al., 1982]). In effect, we have synthesized incident plane wave "shot" records parameterized by slowness, p, and by midpoint.

As neither mode conversion nor multiply reflected energy appears to be important in the data set used for the experiments in this paper, we assumed a primaries only, or single-scattering, approximation. The mechanical parameters are separated into the long-wavelength (smooth) background velocities and density v_P, v_S, and ρ, and short-wavelength relative perturbations of these parameters (reflectivities) $r_P = \delta v_P / v_P$, $r_S = \delta v_S / v_S$, and $r_d = \delta \rho / \rho$. High-frequency asymptotics, leads to the convolutional model approximation to the p-wave seismogram (see [BEYLKIN, 1985]).

$$S(t,p) = f(t,p) * \tilde{r}(t,p)$$

In the above expression, S is the seismogram, f the source wavelet; p denotes slowness, and t time. The "$*$" symbol is convolution in time. The reflectivity $\tilde{r}$ may be written

$$\tilde{r}(t,p) \approx \int dz[A_P(z,t,p)r_P(z) + A_S(z,t,p)r_S(z) + A_d(z,t,p)r_d(z)].$$

The geometric optics reflectivity amplitude A_P is

$$A_P(z,t,p) = \int_{-\infty}^{\infty} d\omega F_P(z,p) \exp\left[i\omega(t - 2\tau(z,p)) - |\omega|\left(1 + \frac{2i}{\pi}\ln|\omega|\right)\alpha(z,p)\right].$$

The vertical travel time of plane waves with slowness, p, is

$$\tau(z,p) = \int_{z_0}^{z} dy \frac{\sqrt{1-(pv_P(y))^2}}{v_P(y)},$$

and

$$\alpha(z,p) = \int_{z_0}^{z} dy \frac{1}{q_P(y)v_P(y)(1-(pv_P(y))^2)^{1/2}}$$

is the corresponding attenuation factor. An algebraic combination of background parameters and slowness gives $F_P(z,p)$. The temporal frequency variable is denoted ω; z_0 is the source depth, and q_P is the p-wave attenuation factor. Similar expressions define the geometric optics amplitudes A_S and A_d. (For a reference to these calculations see [AKI and RICHARDS, 1980].)

Inversion Algorithms

We used two inversion algorithms in our work. The first, output least squares (OLS) inversion, has been described many times in the geophysical literature (see [TARANTOLA, 1987]). In this algorithm, model parameters are adjusted to minimize the mean-square error between predicted (or modeled) and observed data. The parameters of the viscoelastic plane-wave model, as described above, are the background (smooth, long-wavelength) density and wave velocities, the short-scale relative elastic parameter fluctuations (reflectivities), the source parameters, and attenuation profiles. We did not attempt to invert for the attenuation profiles or the background shear velocity or density, relying instead on ad hoc estimates of these parameters. Output least squares inversion for the long-wavelength components of velocity is unlikely to succeed unless the velocity is known with considerable precision prior to inversion ([IGEL, 1993], [SYMES and KERN, 1994] and references listed there). Therefore, we used OLS inversion only to estimate the reflectivities and source, with fixed background and attenuation profiles.

To estimate the background p-wave velocity, v_P, we used a second inversion algorithm, differential semblance optimization (DSO). This modification of OLS inversion also seeks to minimize the misfit between the predicted and observed data. It differs from OLS inversion in the use of an enlarged or infeasible model space. For application to viscoelastic plane-wave inversion this enlargement amounts to allowing the reflectivities to depend explicitly on slowness. That is, each reflectivity is inverted independently for each plane-wave "shot" (i.e., slowness). The p-dependent reflectivity images so produced may be used in the same way as prestack depth migrated image volumes to assess the accuracy of the background velocity. If the velocity is correct, the same events will appear at the same depths independently of slowness. DSO inversion quantifies this idea by adding to the mean-square data misfit a term proportional to the mean-square rate of change of the reflectivity with respect to slowness (differential semblance).

Optimization of the differential semblance objective function produces kinematically accurate background velocities as well as estimates of other model parameters. Algorithmic details are discussed in [SYMES and KERN, 1994]. An application of DSO to marine reflection data in the $p-\tau$ domain based on acoustic (rather than viscoelastic) modeling is presented in [SYMES and CARAZZONE, 1991].

Gulf of Mexico field data set

The data set used here is derived from the seismic survey described in [SYMES and CARAZZONE, 1991]. The geometric specifications of the marine experiment are reproduced here from that paper. The survey consisted of 511 shots collected with a streamer containing 301 hydrophone groups. The group interval was 15m with a minimum source-receiver separation of 148m, and the shot interval was 22.5m. Each group contained 17 equally spaced and equally weighted hydrophones. The data was recorded without a low-cut filter. A 110 Hz high-cut filter was applied. The sampling rate was .002s, and the total record length was 5s. This area of the Gulf contains a strong gas-sand-related direct hydrocarbon indicator (DHI) located near 2.3s readily visible in the stack (see Figure 1 in [SYMES and CARAZZONE, 1991]).

The data were Radon transformed to yield 48 plane-wave traces (per midpoint gather) with slowness values from p_{min}=.1158ms/m to p_{max}=.36468ms/m. A 15 Hz zero-phase Ricker filter was applied to the data to allow a coarser sampling rate to be used. Air gun modeling was used to estimate the source signature and radiation pattern. The anisotropic air gun model for the source was also filtered to match the filtering of the data. This filtered data was used for all experiments except for the one unfiltered data experiment discussed at the end of the next section on velocity estimation.

The numerical experiments described in this paper were performed on a subset of the total number of plane-wave gathers available. In fact we worked with only eleven data gathers which we will refer to as common midpoint data gather (or CMP) 1 through 11. CMP6 (shown in Figure 1) is the midpoint located closest to a logged well. The majority of the experiments were performed on a single gather, most often CMP6.

Numerical experiments

Velocity and elastic parameter estimation

Since the long-wavelength p-wave background velocity determines the kinematics of wave propagation, a very accurate estimate of this parameter is crucial for recovering the depths and details of reflection events. We first inverted for this parameter and for the reflectivities using the DSO inversion algorithm described above. The initial background velocity guess used in the inversion is shown in Figure 2 (dashed/dotted line). It represents a "regional" velocity profile and turns out to be too low. The initial reflectivities were taken to be zeros. For this inversion the fixed source was supplied by the air gun modeling package.

Figure 2 shows both the background velocity estimate obtained after two nonlinear conjugate gradient inversion steps and an estimate of the p-wave background velocity from migration velocity analysis (*MVA*). Figure 3(a) shows the short-wavelength p-wave impedance inversion with the inversion-estimated background velocity (see Figure 2 dark solid line). Figure 3(b) shows the same p-wave impedance resulting from inversion with the MVA velocity shown in Figure 2 (dashed line). One indicator of the accuracy of the background velocity model is its ability to flatten significant events (place them at the same depth) across independent inversions for different image parameters. (See [VERSTEEG and GRAU, 1991] for references to this idea.) As mentioned in the discussion above of DSO inversion, for this application the image ("shot") parameter is the slowness, p. The two panels in Figure 3 show that the MVA and inversion-estimated velocities do a comparable job of flattening the events on the reflectivity panels. The MVA velocity places the main event at about 2200m depth whereas this event is located at about 2150m using the inversion-estimated velocity. From examination of the well log, we believe this event should be located at about 2100m depth.

We were concerned that the velocity estimate not depend on the frequency content of the data. So we performed similar nonlinear inversion experiments with the original data (which had not had the 15 Hz Ricker filter applied). Figure 2 also shows the results of DSO inversion applied to the unfiltered data. One sees that the background velocity estimate from the unfiltered data (solid line) is quite similar to the background velocity estimate from the filtered data (dark solid line).

Elastic parameter and energy source inversion

The second set of inversion experiments were designed to estimate the parameters which have a linear influence on the seismic data, namely the source and the reflectivities. The inversion for source and reflectivity was performed using a method known as coordinate search or alternation (see [MINKOFF and SYMES, 1993]). That is, the source parameters were fixed, and the reflectivities estimated by output least squares inversion. Then the reflectivities were updated and held fixed and the source parameters estimated by OLS inversion. The source is updated and this cycle is repeated until convergence. Alternation, although notoriously inefficient, is attractive for initial experiments because it requires only successive solution of simple linear least-squares problems. Quasi-Newton methods could be applied to the problem and would likely reduce the number of iterations dramatically. The background velocity used throughout the inversion experiments in this subsection was taken to be the inversion estimated background velocity shown in Figure 2 (dark solid line).

For all but the last experiment, the data set was CMP6 (Figure 1). Inversion for the reflectivities alone, using the air gun model source, produced an rms error of 54%.

In contrast, starting from a source guess of an isotropic Ricker wavelet (with peak located correctly in time) and using inversion to alternately estimate the elastic parameters *and the energy source*, we were able to reduce the rms error to 29% in two rounds of alternation.

We also compared our elastic parameter inversion results to an independent measurement, namely the p-wave velocity logs. The logs had been detrended by subtracting a smooth average of the log from the original log and turned into (dimensionless) reflectivities by dividing this difference by the smooth average. Figure 4 shows this comparison. Although the amplitudes have been scaled to correspond and a slight shift in depth applied, the shape of the most significant reflection in the detrended log is well matched by our inversion result.

Finally, we noticed that our assumption of a layered model was not in fact accurate for this data set. Data differences between gathers CMP6 and CMP11 (total offset of 187m) were the same order of magnitude as the actual data. Curious as to how our source and reflectivity estimates would reflect this inaccuracy in our model, we ran one round of alternation using all eleven gathers. Although the source estimates varied considerably between the one-gather experiment and the experiment performed on all eleven gathers, the elastic parameter inversions were remarkably consistent (see Figures 5(a) and 5(b)).

Conclusion

We have applied waveform inversion to a real marine data set from the Gulf of Mexico. This work differs from all previous such studies in at least one of the following four ways: the use of waveform inversion to estimate velocities, the modeling of attenuation, estimation of the energy source parameter via inversion, and correct treatment of three-dimensional amplitudes. The inverted long-wavelength background velocity placed significant reflection events at the same location in depth across a range of slownesses, providing strong evidence of kinematic correctness. Up to a slight shift in depth, our elastic parameter estimates resembled the independent well log measurements. By including energy source estimation in our inversions, we were able to reduce the rms error from 54% to 29%. And, finally, our model appears robust enough not to be dramatically affected by data frequency content or even the incorrect assumption of a layered model.

Acknowlegement: This work was partially supported by the National Science Foundation, the Office of Naval Research, the Texas Geophysical Parallel Computation Project, the Schlumberger Foundation, and The Rice Inversion Project. TRIP Sponsors for 1994 are Advance Geophysical, Amoco Production Co., Conoco Inc., Cray Research Inc., Exxon Production Research Co., Interactive Network Technologies, Mobil Research and Development Corp., and Texaco Inc. We are grateful to Exxon Production Research Co. for provision of the data used in this study and for permission to publish the results.

References

[AKI and RICHARDS, 1980] AKI, K. and RICHARDS, P. (1980). *Quantitative Seismology: Theory and Methods.* Freeman, San Francisco.

[BEYLKIN, 1985] BEYLKIN, G. (1985). Imaging of discontinuities in the inverse scattering problem by inversion of a causal generalized radon transform. *J. Math. Phys.*, 26:99–108.

[IGEL, 1993] IGEL, H. (1993). *Seismic Modeling and Inversion.* PhD thesis, Institut de Physique du Globe de Paris, Paris, France.

[MARTINEZ and MCMECHAN, 1991] MARTINEZ, R. and MCMECHAN, G. (1991). $\tau - p$ seismic data for viscoelastic media – part 1: modelling; part 2: linearized inversion. *Geophysical Prospecting*, 39:141–181.

[MINKOFF and SYMES, 1993] MINKOFF, S. and SYMES, W. (1993). Simultaneous determination of the source-time function and reflectivity via inversion. In *Proc. 63rd Annual International Meeting*, pages 649–652, Washington, D.C., U.S.A. Society of Exploration Geophysicists. Expanded abstract.

[PAN et al., 1993] PAN, G., YOUNG, C., and CASTAGNA, J. (1993). Net pay delineation of gas sand using integrated target-oriented prestack elastic waveform inversion. In *63rd Annual International SEG Meeting*, pages 431–434, Washington, D.C., U.S.A. Society of Exploration Geophysicists. Expanded abstract.

[ROBINSON, 1967] ROBINSON, E. (1967). Predictive decomposition of time series with application to seismic exploration. *Geophysics*, 32:418–484.

[SYMES and CARAZZONE, 1991] SYMES, W. and CARAZZONE, J. (1991). Velocity inversion by differential semblance optimization. *Geophysics*, 56(5):654–663.

[SYMES and KERN, 1994] SYMES, W. and KERN, M. (1994). Inversion of reflection seismograms by differential semblance analysis: Algorithm structure and synthetic examples. *Geophysical Prospecting*, in press.

[TARANTOLA, 1987] TARANTOLA, A. (1987). *Inverse Problem Theory.* Elsevier.

[TREITEL et al., 1982] TREITEL, S., GUTOWSKI, P., and WAGNER, D. (1982). Plane-wave decomposition of seismograms. *Geophysics*, 47:1375–1401.

[ULRYCH, 1971] ULRYCH, T. (1971). Application of homomorphic deconvolution to seismology. *Geophysics*, 36:650–660.

[VERSTEEG and GRAU, 1991] VERSTEEG, R. and GRAU, G. (1991). Practical aspects of inversion: The Marmousi experience. Proceedings of the EAEG, The Hague.

[WOOD, 1993] WOOD, W. (1993). Linearized least-squares inversion of field seismic data for an elastic 1-d earth. In *63rd Annual International SEG Meeting*, pages 661–664, Washington, D.C., U.S.A. Society of Exploration Geophysicists. Expanded abstract.

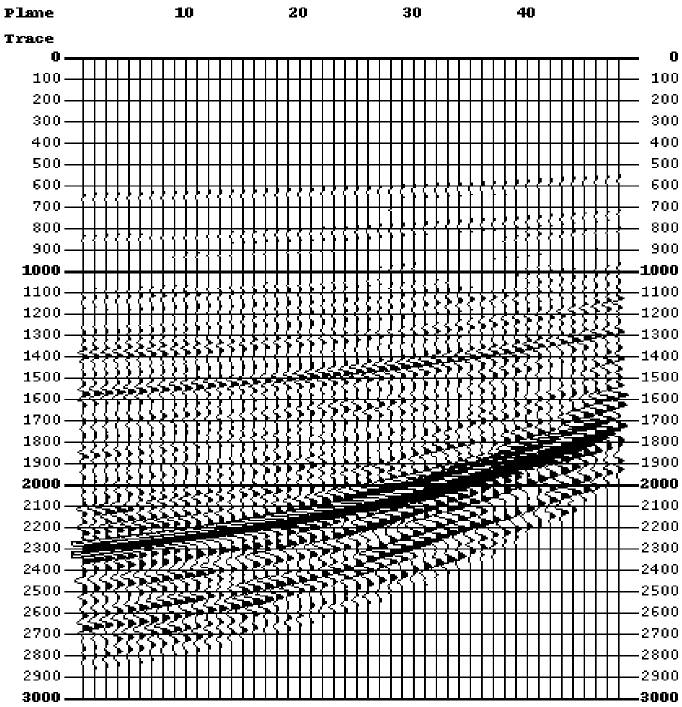

FIGURE 1: The seismic data from common midpoint gather 6 after convolution with a 15 Hz Ricker wavelet filter.

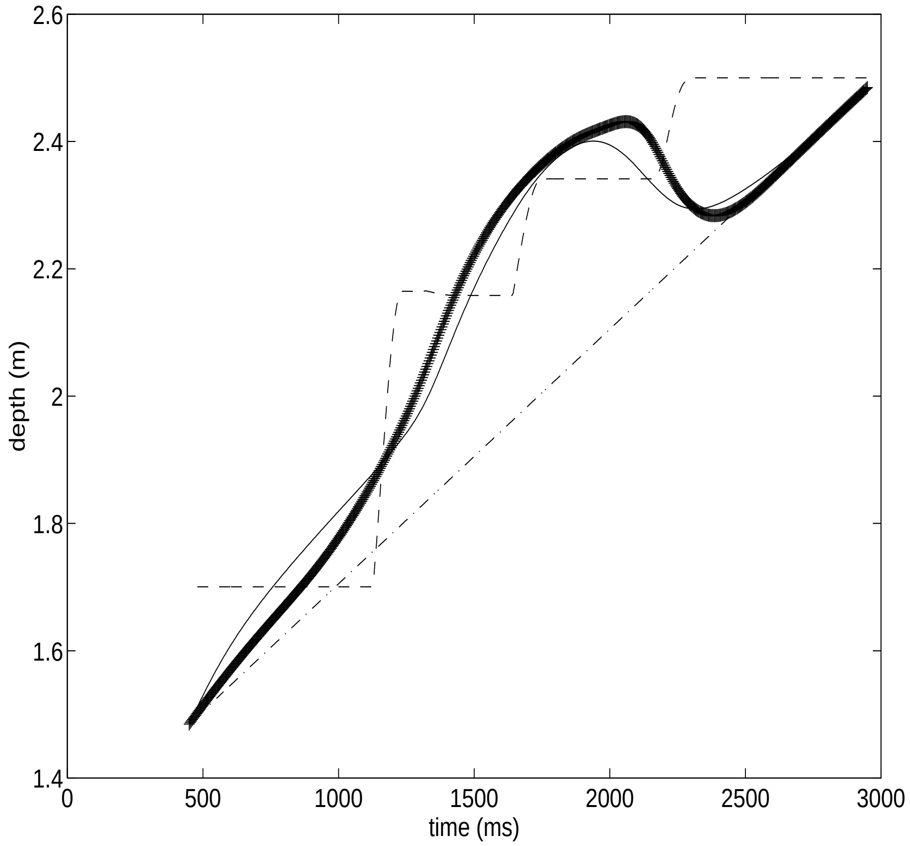

FIGURE 2: Dashed/dotted line: Initial estimate for P-wave background velocity used for inversion of common midpoint data gather 6. Dashed line: Background velocity predicted for the same data set using migration velocity analysis. Solid line: P-wave background velocity determined via inversion for *unfiltered* CMP6. Dark solid line: Background velocity estimate gotten from performing the same inversion on *filtered* CMP6 data.

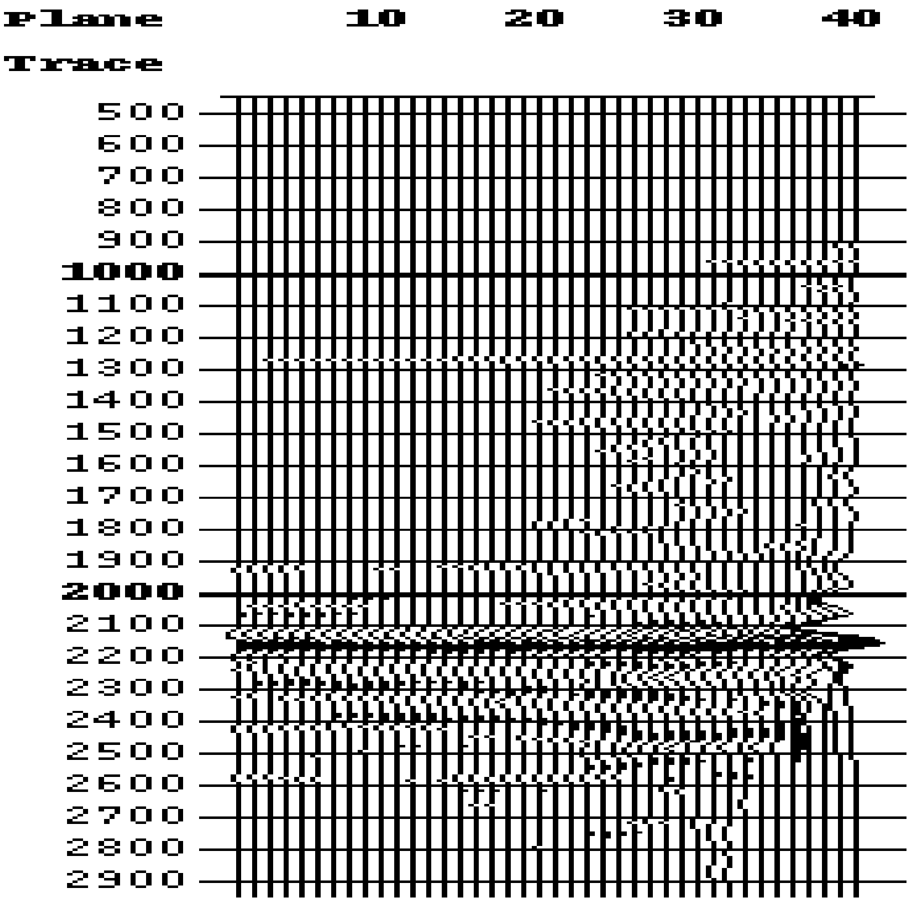

FIGURE 3(a): P-wave impedance resulting from an inversion using the inversion-estimated background velocity shown in Figure 2 (dark solid line).

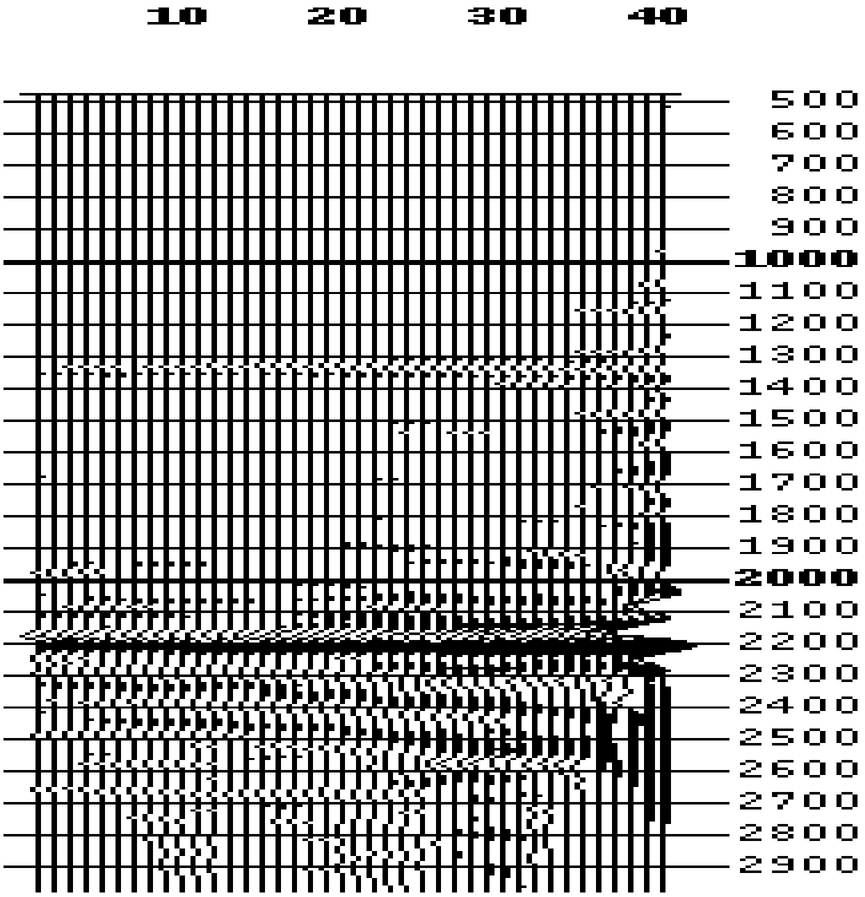

FIGURE 3(b): P-wave impedance resulting from an inversion using the migration velocity analysis background velocity shown in Figure 2 (dashed line).

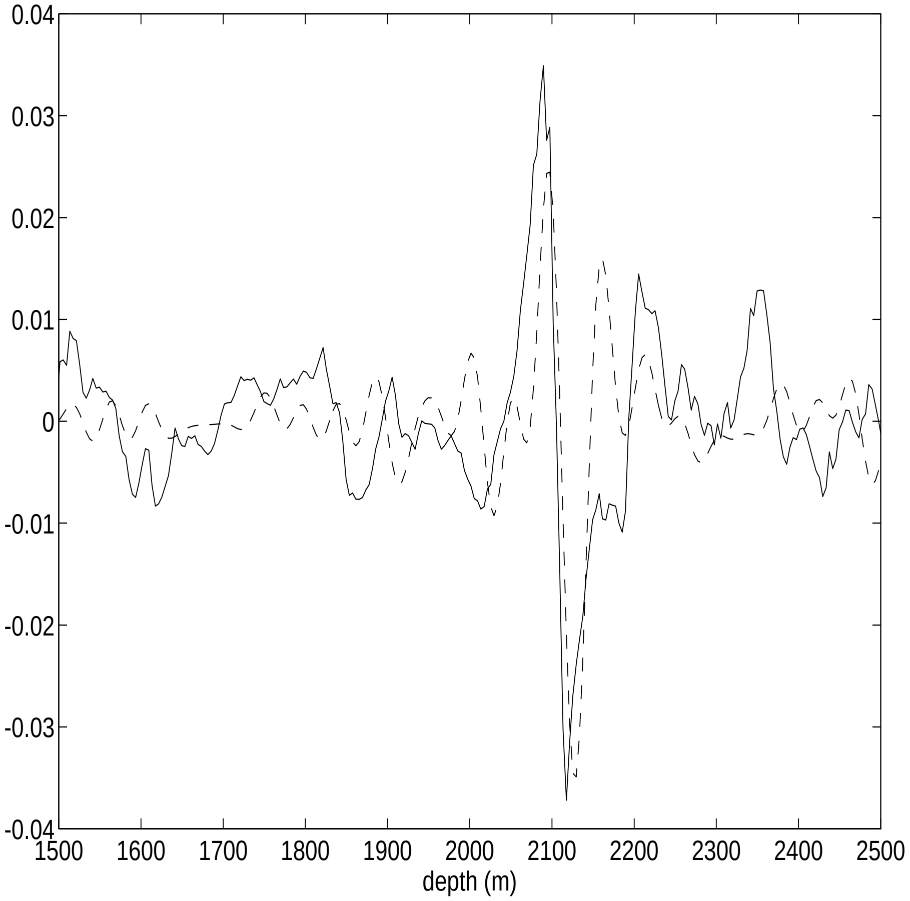

Figure 4: Comparison of the detrended well-log measurement of the p-wave velocity with the result of inversion done on CMP6. The solid line shows the well log vp. The dashed line shows the inversion result. The dashed graph has been scaled to match the peak value of the log, and a shift of 56 meters to the left has been applied.

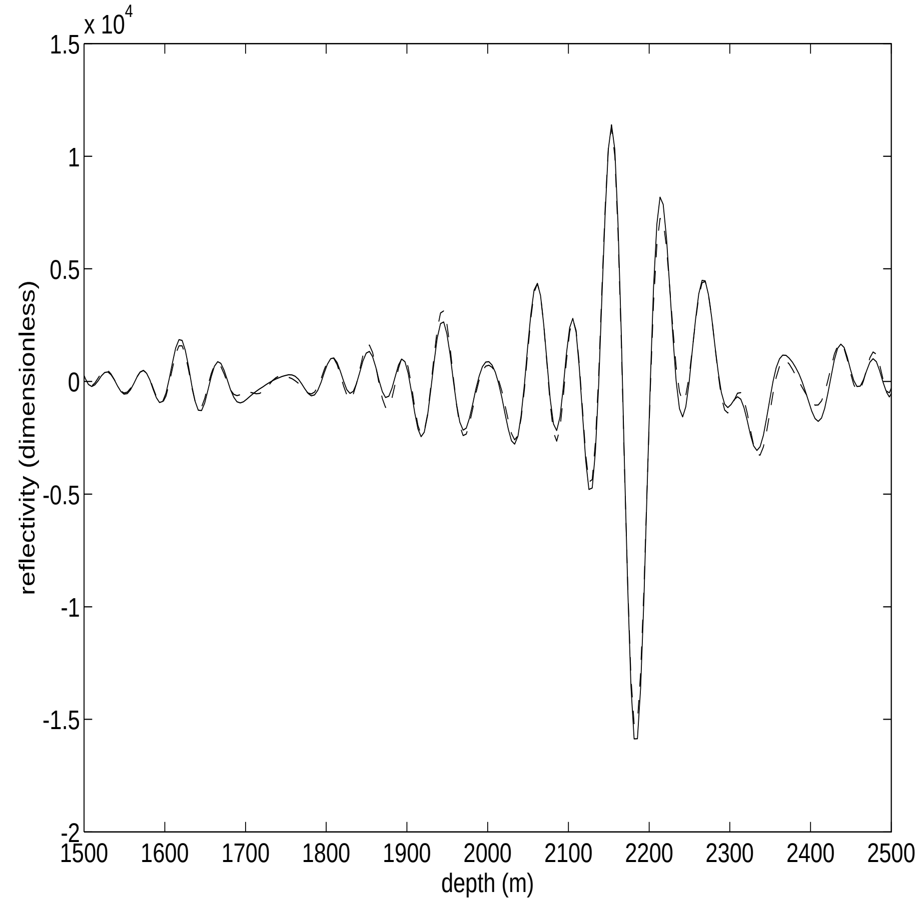

FIGURE 5(a): The short-scale relative p-wave impedance fluctuation (reflectivity) results from two different inversion experiments. The solid line was the result of inverting only single gather CMP6. The dashed line resulted from performing an inversion on all eleven gathers.

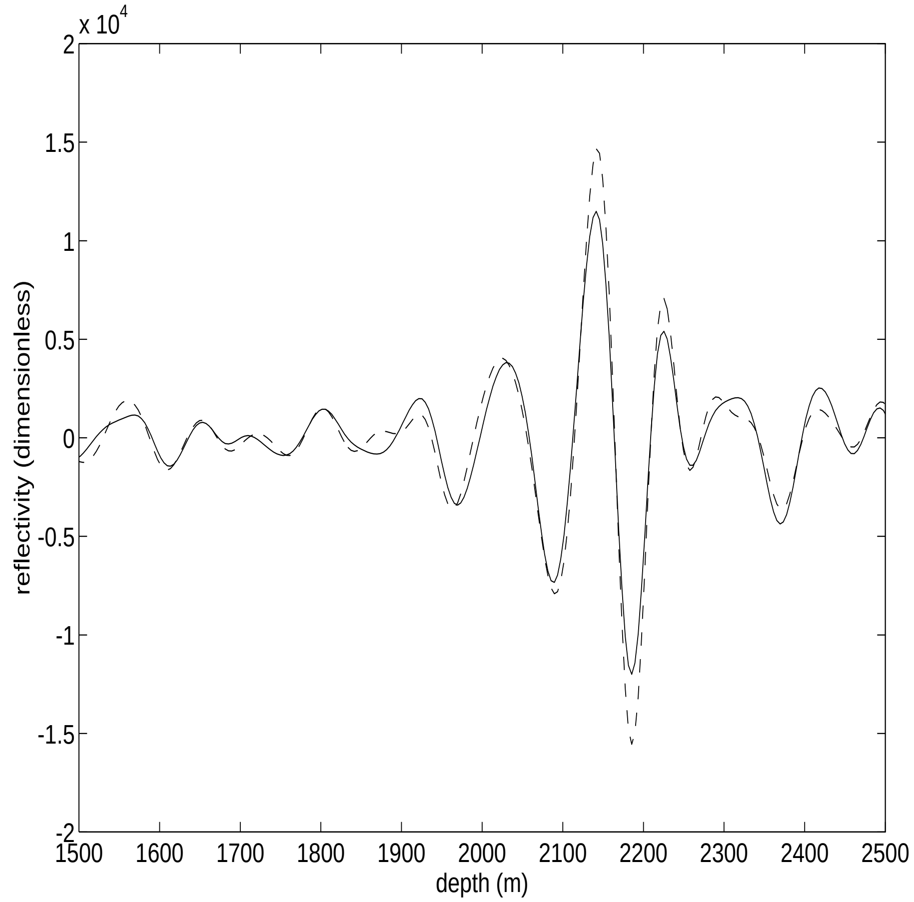

Figure 5(b): The short-scale relative fluctuation in the p-wave velocity divided by density. The solid line was the result of inverting only single gather CMP6. The dashed line is the same elastic parameter gotten by performing the inversion on all eleven gathers.